Removal of CO$_2$ using Poly(4-methyl-1-pentene) non-porous hollow fiber membranes as permabsorbers

H.Y. ZHANG[a], R.WANG[b], D.T. LIANG[b], J. H. TAY[a,b]
a. School of Civil and Environmental Engineering
b. Institute of Environmental Science & Engineering
Nanyang Technological University
Innovation Center (NTU), Block 2, Unit 237, 18 Nanyang Drive
SINGAPORE 637723

Abstract: - Nonporous PMP hollow fiber modules were used as permabsorbers for the application of CO$_2$ removal from CO$_2$/N$_2$ mixtures through integrated permeation and absorption approach. The permabsorber was experimentally and theoretically investigated under different operating conditions using distilled water and 2M aqueous DEA solutions as absorbents. It was found that experimental data were in an excellent accordance with the results predicted from the mathematical model, which used the experimentally determined membrane permeance to characterize the mass transfer resistance imposed by the dense layer of the membrane. In the case of water used as the absorbent, the mass transfer resistance mainly lied in the liquid phase. Resistance from dense layer only accounts for less than 20% of the total mass transfer resistance. In the case of 2M aqueous DEA solutions as the absorbent, the resistance in liquid phase can be significantly reduced due to the fast reaction between CO$_2$ and DEA. The CO$_2$ flux increased with an increase in the gas inlet velocity. Though the mass transfer resistance introduced by the dense membrane layer took a proportion as high as 40%~80% of the overall mass transfer resistance, a remarkable CO$_2$ absorption flux was still obtained.

Key-words: - CO$_2$ removal; permabsorber; modeling; mass transfer resistance; permeation; absorption

1 Introduction

Despite increased use of renewable energy sources, approximately 80% of the primary energy used today is based on fossil fuels. However, the combustion of fossil fuels inevitably results in the emissions of air pollutants and huge release of carbon dioxide (CO$_2$) that has been considered as one of the main greenhouse gases (GHG). CO$_2$ capture from various gas streams, particularly from flue gas, has attracted extensive attentions.

Several techniques are available for the separation of CO$_2$ from flues gas streams. The process of membrane modules integrated with chemical absorption is one of research focuses because of its advantages over the traditional gas absorption processes. For CO$_2$ transfer through the membrane in this combined process, the membranes used can either be mircoporous or non-porous. The former is normally called as membrane contactors and the latter is referred to membrane permabsorbors, where the porous or non-porous polymeric membranes serve as the contacting media to separate liquid phase and gas phase from each other, thus avoiding the problems often encountered in the conventional apparatus such as flooding, foaming and entrainment.

With rapid development of polymetric membrane fabrication techniques, it is possible to produce ultrathin gas-permeable polymeric membranes at present, which has stimulated research to evaluate their utilization as the membrane permabsorbors in gas-liquid contacting systems [1-2]. In this paper, a numerical simulation was performed to describe both physical and chemical absorptions of CO$_2$ from a CO$_2$/N$_2$ mixture in Poly(4-methyl-1-pentene) (PMP) non-porous hollow fiber modules. The distribution of liquid velocity in the shell side was taken into account in the modeling. The corresponding experiments were also carried out to verify simulated results in

order to gain a better understanding of the membrane permabsorbers used for CO_2 capture.

2   Theory

2.1 Reaction mechanism

Zwitterion mechanism has been commonly accepted as the reaction mechanism between CO_2 and primary or secondary amines. The rate of CO_2 reaction with DEA was derived as [3]:

$$r_A = \frac{[DEA][CO_2]}{\dfrac{1}{k_2} + \dfrac{1}{\dfrac{k_2 k_{H_2O}}{k_{-1}}[H_2O] + \dfrac{k_2 k_{OH^{-1}}}{k_{-1}}[OH^{-1}] + \dfrac{k_2 k_{DEA}}{k_{-1}}[DEA]}} \quad (1)$$

2.2 Model development

The schematic diagram of liquid and gas flows in a hollow fiber is shown in Fig.1. The liquid absorbent was assumed to flow in the shell of the membrane while the gas mixture of CO_2/N_2 flows in the lumen side co-currently. Following assumptions have been adopted: (1) a steady state and isothermal condition have been achieved; (2) the axial diffusion is negligible; (3) a fully developed parabolic liquid velocity profile is presented within the lumen of the hollow fiber; (4) ideal gas behavior for gas phase; (5) constant gas permeability; and (6) Henry's law is applicable.

2.2.1 Mass transfer in the liquid phase

Based on above assumptions, the conservation equation for the mass transfer in the liquid phase can be written as:

$$v_z \frac{\partial C_A}{\partial z} = D_A \frac{\partial^2 C_A}{\partial r^2} + \frac{D_A}{r} \frac{\partial C_A}{\partial r} - r_A \quad (2)$$

$$v_z \frac{\partial C_B}{\partial z} = D_B \frac{\partial^2 C_B}{\partial r^2} + \frac{D_B}{r} \frac{\partial C_B}{\partial r} - r_B \quad (3)$$

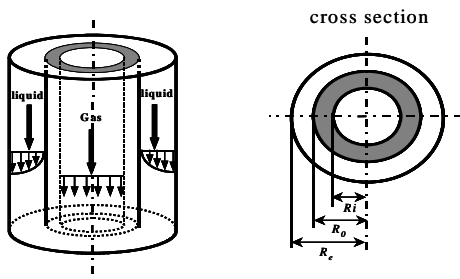where the subscripts of A and B denote CO_2 and DEA respectively.

Fig. 1 Schematic diagram of liquid and gas flows in a hollow fiber

The liquid flow in the shell side of the membrane contactor can be configured as a fluid envelope around the fiber and there is no interaction between fibers. The dimension of the free surface can be estimated by Happel's free surface model [4]:

$$R_e = (\frac{1}{1-\varepsilon})^{1/2} R_0 \quad (4)$$

The liquid axial velocity profile is given by the Happel's free surface model:

$$v_z = 2U_L[1-(\frac{R_0}{R_e})^2] \times [\frac{(r/R_e)^2 - (R_0/R_e)^2 + 2\ln(R_0/r)}{3 + (R_0/R_e)^4 - 4(R_0/R_e)^2 + 4\ln(R_0/R_e)}] \quad (5)$$

The initial and boundary conditions are

$$z = 0, \ C_A = 0, \ C_B = C_{B0} \quad (6)$$

$$r = 0, \ \frac{\partial C_A}{\partial r} = 0, \ \frac{\partial C_B}{\partial r} = 0 \quad (7)$$

$$r = R_0, \ C_A = HC_{AM,R_i}, \ \frac{\partial C_B}{\partial r} = 0 \quad (8)$$

where a symmetry in the radial direction of hollow fibers and non-volatile DEA are assumed. The Henry's law is applied to connect CO_2 interfacial concentrations in the liquid and membrane phase. The physical properties of CO_2 in water and 2M aqueous DEA solutions were cited or calculated with the methods introduced in the reference [5].

2.2.2 Mass transfer in the gas phase

Considering that the CO_2 diffusivity in gas phase is much higher than that in liquid phase, it is reasonable to assume the gas flow as plug flow, which implies that the gas velocity and concentration distributions in the radial direction can be ignored in the lumen side of the fiber. For a segment with a length of Δz in the axial direction, the mass balance can be written as:

$$\Delta n_{AG} = C_{AG} \Delta U_G A_G + \Delta C_{AG} U_G A_G + \Delta C_{AG} \Delta U_G A_G \quad (9)$$

Under the operation pressure (normal pressure), the ideal gas law is applied to the gas phase:

$$\frac{P}{RT} \cdot \Delta U_G A_G = \Delta n_{AG} \quad (10)$$

Combining Eqs. (9) and (10), the CO_2 removal rate in the segment can be derived as:

$$\Delta n_{AG} = \frac{\Delta C_{AG} U_G A_G}{1 - \dfrac{RT}{P} \Delta C_{AG} - \dfrac{RT}{P} C_{AG}} \quad (11)$$

2.2.3 Mass transfer in the membrane phase

In the membrane phase, the mass transfer rate in a segment with a length of Δz can be expressed by:

$$\Delta n_{AM} = (\frac{P}{\delta}) \cdot (RT) \cdot (C_{AG,av} - C_{AM,R})(2\pi R_0 \Delta z) \qquad (12)$$

where Δn_{AM} is equal to Δn_{AG} based on mass conservation. In addition, the overall mass transfer coefficient can be calculated according to:

$$K_{OG} = \frac{\Delta n_{AT}}{\Delta p_{av} A_T} \qquad (13)$$

The logarithmic mean concentration, Δp_{av}, is given by:

$$\Delta p_{av} = \frac{(p_{AG,in} - p_{AL,in}) - (p_{AG,out} - p_{AL,out})}{\ln(\frac{p_{AG,in} - p_{AL,in}}{p_{AG,out} - p_{AL,out}})} \qquad (14)$$

2.3 Numerical scheme

Along the axial direction, the fiber was divided into many small segments with an equivalent length of Δz. Firstly, a method of line was applied to reduce the partial differential equations to ordinary differential equations. Then, by giving a guessed value of the gas phase CO_2 concentration at the outlet of the first segment, Δn_{AG} and $C_{AM,R}$ were calculated via Eqs.11 and 12. The ordinary differential equations can be solved with their initial and bondary conditions, which contained $C_{AM,R}$ using MATLAB.

After obtaining the concentration profiles of CO_2 and DEA at the inlet and outlet of the segment, the CO_2 mass transfer rate Δn_{AL} in the liquid phase can be calculated by integrating the CO_2 concentration along the radial direction. Since CO_2 loss in the gas phase (Δn_{AG}) should be equal to the gain in the liquid phase (Δn_{AL}), the initially guessed value of the gas phase CO_2 concentration at the outlet of the first segment was adjusted until the difference between Δn_{AG} and Δn_{AL} was acceptable. Similar procedures were taken to calculate the following segments.

3 Experimental

3.1 permeance test of pure gases

The PMP hollow fibers were mounted into a glass module with two ends sealed with epoxy. Each of the pure gases, CO_2, O_2 and N_2 was fed into the shell side of the glass membrane module.

The total flow from the lumen side of the hollow fibers was measured at one atmosphere and 25 °C after being stable. Considering that the absorption experiment is operated at normal pressure and the strength of glass material is limited, the feed gas pressure is controlled under 250 KPa. The permeance was calculated using the following equation:

$$(\frac{P}{\delta}) = (\frac{N}{2n\pi R_0 L \Delta p})(\frac{273.15}{T}) \qquad (15)$$

3.2 Permabsorption

PMP 200 hollow fibers, which were kindly provided by Celgard Inc., were used to make the membrane permabsorbor. A 99.5% grade DEA purchased from Merck was dissolved in distilled water to prepare aqueous 2M solutions.

The experimental setup can be found elsewhere [6]. A CO_2/N_2 mixture with a volume ratio of 20/80 was used as the feed gas while the N_2 saturated distilled water or aqueous 2M DEA solutions were used as the absorbents. In this study, the liquid always passed through the shell-side and the gas flowed co-currently through the lumen side of the hollow fibers. The details of experimental procedures were described in [6].
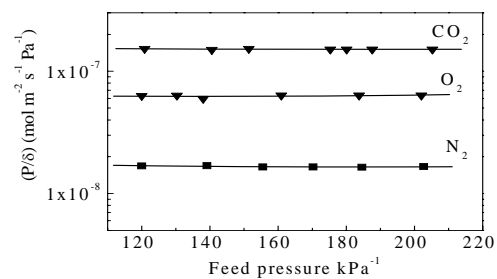

Fig. 2 Pure gas permeance through PMP hollow fiber membranes

4 Results and discussion

4.1 Permeability of PMP membranes

The experimentally determined permeance of pure gases of CO_2, O_2 and N_2 in the non-porous PMP hollow fibers are plotted against the feed pressure in Fig. 2. From the figure, it can be seen that the permeance of the three gases was kept almost constant over the pressure range tested. The effect of feed pressure on the permeance is negligible, which verifies the validity of the assumption of constant permeance over the operating pressure.

The permeance of CO_2 through the membrane can also be calculated from the permeation and absorption model in combination with the absorption experiment. By giving an assumed value of membrane permeance P/δ in Eq. (12) and following the numerical schemes, the CO_2 mass transfer rate at each segment Δn_{AL} can be obtained. The summation of all the Δn_{AL} leads to the acquirement of total CO_2 transfer rate Δn_{AT}, which actually can be determined by the absorption experiment. Thus, the membrane permeance can be finally acquired by adjusting the initially guessed value of P/δ to make the difference of the calculated and measured Δn_{AT} being sufficiently small. The value of CO_2 permeance obtained using this approach is 1.32×10^{-7} mol m^{-2} s^{-2} Pa^{-1}, which is reasonably consistent with the experimental value of 1.55×10^{-7} mol m^{-2} s^{-2} Pa^{-1}.

4.2 Permeation and physical absorption

Fig. 3 shows the theoretical and the experimental results of CO_2 flux (J_{CO2}) versus liquid velocity (U_L) using distilled water as the absorbent. It can be seen that J_{CO2} increased with the increase of liquid velocity and the theoretical results agreed well with the experimental data. However, no visible effects of the inlet gas velocity on J_{CO2} were observed.
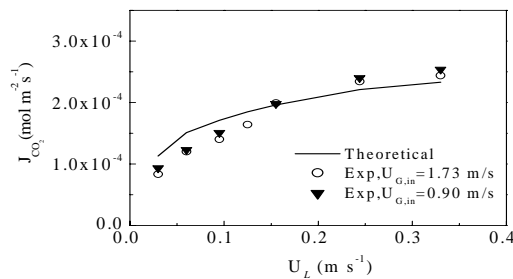

Fig.3 CO₂ flux using distilled water as the absorbent

When non-porous membranes are used as gas-liquid contacting media, an extra resistance was introduced into the process inevitably. Fig.4 shows the proportion of mass transfer resistance caused by the membrane. The mass transfer resistance imposed by the membrane dense layer was less than 20% of the total mass transfer resistance over the liquid velocity range studied in the case of physical absorption. Apparently,

the mass transfer resistance mainly existed in the liquid phase and the performance of CO_2 capture was not affected significantly by the introduction of the non-porous dense layer of the hollow fibers.
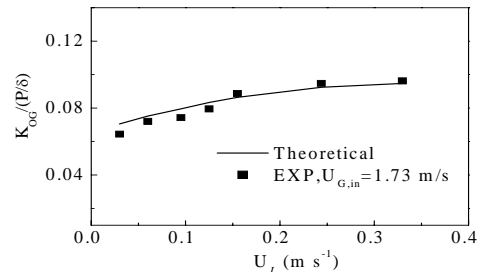

Fig. 4 Proportion of membrane resistance in the overall mass transfer resistance (distilled water)

4.3 Permeation and chemical absorption

In the case of 2M aqueous DEA solutions being used as the absorbent, the solubility of CO_2 in liquid phase is greatly improved by the chemical reaction between CO_2 and DEA, leading to a higher CO_2 absorption rate. The effect of liquid velocity on CO_2 flux is presented in Fig. 5.
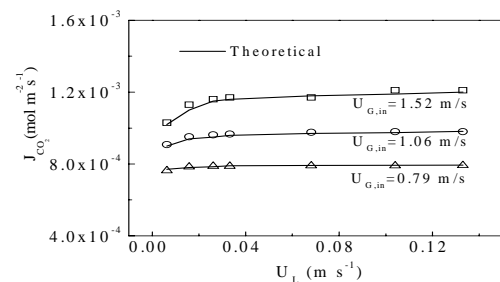

Fig. 5 CO₂ flux as a function of absorbent flow rate (2M aqueous DEA solutions)

It is noticed that the CO_2 flux changed with the liquid velocity in a way different from that of physical absorption. In the regime of very low liquid velocity, the CO_2 absorption flux increased with the liquid velocity, whereas in the regime of relatively high liquid velocity, the CO_2 flux was almost not affected by the liquid velocity. This is probably due to the significant depletion of active amines in the solution at low liquid velocities. With an increase in the liquid velocity, the supply of the active amines was accelerated and the depletion could be mitigated effectively. Since the high velocity regime is ideally suitable for the operation of membrane

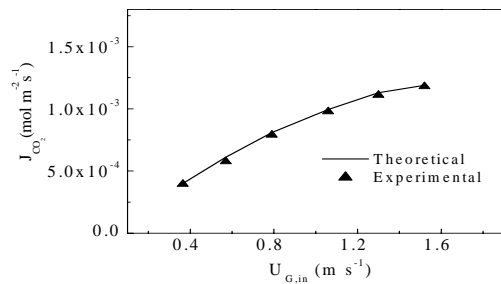permabsorbors and therefore, our subsequent studies are focused on this regime.

Fig. 6 CO_2 flux as a function of inlet gas flow rate (2M aqueous DEA solutions)

The impact of inlet gas velocity on the CO_2 flux (J_{CO2}) is depicted in Fig 6. Modeling results suggested that the increase of gas velocity could effectively enhance the CO_2 mass transfer, which was confirmed by the experiments. As shown in the figure, the CO_2 flux through the non-porous membrane was accelerated by the feed gas velocity. The faster the gas mixture was fed into the permabsorber, the higher the CO_2 flux. For the chemical absorption in the nonporous membrane module, the CO_2 absorption rate was mainly determined by the chemical reaction rate as the membrane resistance was remained constant. Our earlier study showed that with DEA concentration as high as 2M, except the regime close to the gas-liquid interface, most of amine solutions are still intact in the liquid phase and the overall depletion of DEA can be neglected compared with that of CO_2 in gas phase [6]. Thus the reaction is mainly determined by the CO_2 concentration at the gas-liquid interface. When the feed gas was introduced into the system, the higher the inlet gas velocity, the higher the average CO_2 concentration in the gas phase, leading to a bigger amount of CO_2 permeating through the membrane and a higher CO_2 concentration at the gas-liquid interface. Therefore, more CO_2 absorption can be achieved by increasing feed gas velocity.

Fig. 7 shows the proportion of the dense layer resistance varying with gas velocity. It occupied less than 50% of the overall resistance at a relatively low gas velocity regime. With the increase of gas velocity, the proportion might be

close to 80%. Compared with the case using water as the absorbent, the resistance of the dense layer accounted for a much higher proportion of the overall mass transfer resistance. This is because the resistance in the liquid phase can be significantly decreased by the chemical reaction between CO_2 and DEA, which made the resistance introduced by the dense membrane layer being more pronounced. Nevertheless, though the dense membrane layer introduced an extra resistance, the CO_2 flux was still much higher than that of using distilled water as absorbent and the reduction by the dense layer may be remedied by the high-pressure operation.
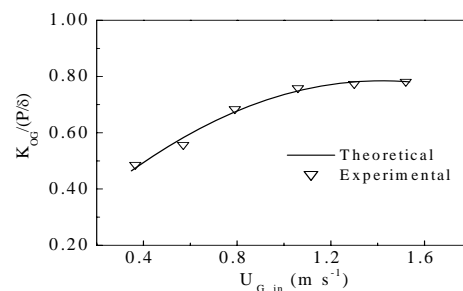

Fig. 7 Proportion of membrane resistance in the overall mass transfer resistance (2M aqueous DEA solutions)

5 Conclusions

A non-porous PMP hollow fiber permabsorber was experimentally and theoretically investigated for CO_2 removal from CO_2/N_2 mixtures by using distilled water and 2M aqueous DEA solutions as absorbents under different operating conditions. Experimental data agreed well with the results predicted from the mathematical model, which used the experimentally determined membrane permeance to characterize the mass transfer resistance imposed by the dense layer of the membrane.

For water used as the absorbent, the mass transfer resistance mainly lied in the liquid phase. Resistance from dense layer only accounts for less than 20% of the total mass transfer resistance. Therefore, CO_2 flux across the membrane can be effectively improved by increasing the liquid velocity. For 2M aqueous DEA solutions as the absorbent, the resistance in liquid phase can be significantly reduced due to the fast reaction between CO_2 and DEA. At a relatively high liquid velocity, CO_2 flux did not increase with liquid velocities since the overall depletion of DEA is small and DEA

concentration almost kept constant in the liquid phase. In contrast, CO_2 flux increased with the gas inlet velocity, because the average CO_2 concentration in the gas phase can be improved by increasing the gas inlet velocity, leading to a faster reaction in the liquid phase. Compared with using water as the absorbent, the resistance from the dense membrane layer took a proportion as high as 40%~80% of the overall mass transfer resistance, but a remarkable CO_2 absorption flux was still obtained.

Nomenclature

A_G cross sectional area for gas flow in a mass transfer segment, m^2

C_A, C_{AG} concentrations of carbon dioxide in liquid and gas phases, $mol\ m^{-3}$

C_{AM} concentration of carbon dioxide in membrane phase, $mol\ m^{-3}$

C_B, C_{B0} concentrations of DEA in liquid phase, at inlet, $mol\ m^{-3}$
          concentration of DEA in liquid phase

D_A, D_B diffusion coefficients of CO_2, DEA in liquid phase, $m^2\ s^{-1}$

H Henry's constant, $(H=[CO_2]_l/[CO_2]_g$ at equilibrium) (-)

J_{CO_2} absorption flux of CO_2, $mol\ m^{-3}\ s^{-1}$

L, L_{eff} fiber length and effective mass transfer length of hollow fiber, m

$\Delta n_A, \Delta n_{AT}$ carbon dioxide mass transfer rates in a segment and in all the segments, $mol\ s^{-1}$

P operation pressure in gas phase in Eq. (10-11), Pa;
          permeability of pure gases through non-porous membrane in Eq. (12)

P/δ permeance of pure gases through non-porous membranes, $mol\ m^{-2}\ s^{-1}\ Pa^{-1}$

p partial pressure of CO_2, Pa

r radial coordinate, m

r_A, r_B reaction rates of CO_2, DEA, $mol\ m^{-3}\ s^{-1}$

R gas constant, $8.314\ Jmol^{-1}K^{-1}$

R_i internal radius of a hollow fiber, m

R_0 radius of gas free surface, m

R_e external radius of a hollow fiber, m

T operating temperature, K

U_L average liquid velocity, $m\ s^{-1}$

$U_{G,in}$ gas velocity at the inlet, $m\ s^{-1}$

v_z liquid velocity in axial direction at radial position of r, $m\ s^{-1}$

z axial coordinate, m

Δz length of a mass transfer segment, m

ε shell-side void volume fraction of a hollow fiber module

Subscripts

A carbon dioxide

av average

B diethanolamine

G gas phase

in inlet

L liquid phase

M membrane phase

out outlet

References:
[1] A.B. Shelekhin and I.N. Beckman, Gas processes in membrane absorber, *J. Membr. Sci.* 73, 1992, pp. 73-85.

[2] K. Li, Y. Chen, W.K. Teo, Removal of CO_2 from a breathing gas mixture using a hollow-fibre permeator with permeate purge and absorption, *Gas. Sep. Purif.*, 9, 1995, pp. 93-100.

[3] G. F. Versteeg and M.H. Oyevaar, The reaction between CO_2 and diethanolamine at 298 K, *Chem. Eng. Sci.*, 44, 1989, pp. 1264-1268.

[4] J. Happel, Viscous flow relative to arrays of cylinders, *AIChE J.*, 5, 1959, pp. 174-177.

[5] G. F. Verteeg and W. P. M. van Swaaij, Solubility and diffusivity of acid gases (CO_2, N_2O) in aqueous alknolamine solutions, *J. Chem. Eng. Data,* 33, 1988, pp. 29-34.

[6] H.Y. Zhang, R. Wang, D.T. Liang, J.H. Tay, Modelling and experimental study of CO_2 absorption in hollow fiber membrane contactors. *J Membr. Sci.,* 279 2006, pp. 301–310.